Publishing House
AKAPIT

COMPUTER METHODS IN MATERIALS SCIENCE
Informatyka w Technologii Materiałów

Vol. 15, 2015, No. 3

THERMAL-MECHANICAL-MICROSTRUCTURAL MODEL OF ROLLING AND COOLING OF RAILS

GRZEGORZ SMYK*, MONIKA PERNACH, MATEUSZ AMBROZIŃSKI

AGH University of Science and Technology, al. Mickiewicza 30, 30-059 Kraków, Poland
**Corresponding author: grzegorz.smyk@agh.edu.pl*

Abstract

The paper describes complex thermal-mechanical-microstructural model of rolling and cooling of rails. The equations describing microstructure evolution and phase transformations in rail steels were implemented in the Finite Element code, which simulates thermal and mechanical phenomena. Numerical tests of the model were performed. Simulations covered last three passes of the rolling process followed by controlled cooling of the rail head. The results included changes of the temperature during the whole manufacturing cycle, as well as changes of the austenite grain size during rolling and kinetics of the phase transformations during cooling. Numerical tests confirmed good predictive capabilities of the model.

Key words: pearlitic steels, rails, controlled cooling, modelling, validation

1. INTRODUCTION

The constant development of rail transport is specifically connected with an increase in train speed, application of greater axle loads due to an increase in the weight of materials carried by rail transport, as well as linking of the railway networks with the tram infrastructure. Over the last decades a constant progress has been made in the rail transportation sector. The rail transport capacities depend strongly on such track parameters as car stability, geometry of the contact with running wheel, and possibility to sustain greater loads (Kuziak & Zygmunt, 2012). Quality of rails is characterized by the increased wear resistance, fatigue strength and resistance to contact-fatigue defects occurrence. This features can be obtained for the pearlite structure after accelerated cooling with small distance between the cementite lamellae (S_0 around 0.10-0.12μm), as compared to the structure after the natural cooling in the air (S_0 around 0.2-0.3 μm) (Kuziak & Zygmunt, 2012). Reduction of the distance between lamellae results in an increase of pearlite strength/hardness (Kuziak et al., 1997; Kuziak & Zygmunt, 2012). Simultaneously, it results in thinning of cementite lamellae, which increases plasticity of this phase.

Problem of heat treatment of rails directly after hot rolling has been in the field of interest of scientist for some time. Numerous papers dealing with the phenomena of heat transfer (Ackert & Nott, 1987; Morales et al., 1990; Sahay et al., 2009) microstructure evolution (Perez-Unzueta & Beynon, 1993) and thermal stresses (Boyadiev et al., 1996) can be found in the scientific literature. Intensive researches, aimed at designing of new method of pearlitic rails head hardening process giving rise to substantial progress in reducing of the interlamellar spacing of cementite lamellae and the size of pearlite colony as compared to the these parameters after cooling in still air, have been conducted by (Kuziak & Zygmunt, 2012). Physical simulations of the controlled cooling system designed by (Kuziak & Zygmunt, 2012) were performed in (Kuziak et al., 2014). Beyond this, various researchers have developed models describing kinetics of phase transformation for

 ISSN 1641-8581

eutectoid steels to be adopted into the continuous cooling conditions using additivity rule. These models allow description of such features of the austenite decomposition in eutectoid steels as the transformations start and end temperature, as well as volume fractions of structural components. Application of models based on solution of the diffusion differential equation allows accounting for arbitrary changes of the temperature (Pernach, 2014). More advanced models can predict such specific features of the pearlitic microstructure as grain size, colony size and interlamellar spacing, see for example (Pietrzyk & Kuziak, 2000). This model was applied by (Pietrzyk & Kuziak, 2012) to simulation of controlled cooling of rail head.

Discussed models focus mainly on phase transformations during cooling. Separately researchers were developing models combining thermal-mechanical FE code with equations describing microstructure evolution during hot rolling of rails (Głowacki, 2000; Ma et al., 2014). The main objective of this paper was combining models for rolling and cooling and development of the thermal-mechanical-microstructural model for the whole manufacturing cycle for rails.

2. MODELLING OF ROLLING AND COOLING OF RAILS

All models, which were used in simulations of the rolling-cooling sequence, are described in this Chapter. The models are general but all the coefficients in these models were obtained for the pearlitic steel 900A containing 0.71%C, 1.05%Mn, 0.31%Si, and 0.03%Cr.

2.1. Thermal-Mechanical model of rolling and cooling

Rolling of rails requires fully 3D simulations, which are time consuming. Since this process is composed of several passes, problem of computing costs becomes particularly important. Therefore, researchers have been searching for the simplified approach, which will allow maintaining the accuracy of simulation on a reasonable level. In the mechanical part of the model so called generalised plane-strain approach (2.5D) appeared to be very efficient (Głowacki, 1996). This approach simplifies the strain and strain rate tensors and significantly saves computing time and computer memory requirements without decreasing accuracy of the solution. The main assumption of the theoretical model is the decomposition of the process into several steps related to subsequent material locations in the roll gap. It is assumed that the strain tensor components related to the rolling direction are distributed uniformly across the sample cross-section, which is perpendicular to the rolling axis. This assumption results in constant strains and strain rates in the rolling direction and it reduces the related to that direction shear components of strain and strain rate tensors. Only a cross-section of the strip is analysed using non-steady state approach keeping in mind that the whole process is spatial. In the thermal part of the model 2.5D assumption leads to neglecting of the conduction along the rail. 2.5D approach was combined with the microstructure evolution model and became very efficient tool for simulations of rail rolling (Głowacki, 2000; 2005).

Significant increase of the computing power during last decade allows now fully 3D simulation of rail rolling, which involves reasonable computing times (Pei et al., 2014). Much of effort was put on modelling of the rolling contact fatigue (RCF) and crack growth (Wen et al., 2011; Pletz et al., 2014), which are now crucial problems from the point of safety of passengers. These phenomena were also considered also by (Garnham & Davis, 2011) and by (Franklin et al., 2011), who performed 3D modelling of rail steel microstructure as well as crack initiation and propagation. In the present paper 3D simulations of rolling are performed to supply data regarding the state of the microstructure at the beginning of controlled cooling.

3D FE code ABAQUS was used in thermal-mechanical simulations of rail rolling. The constitutive law was based on the rigid-plastic Levy-Mises flow rule:

$$\boldsymbol{\sigma} = \frac{2\sigma_p}{3\dot{\varepsilon}_i}\dot{\boldsymbol{\varepsilon}} \tag{1}$$

where: $\boldsymbol{\sigma}$, $\dot{\boldsymbol{\varepsilon}}$ – stress and strain rate tensors, σ_p - flow stress, $\dot{\varepsilon}_i$ - effective strain rate.

Flow stress in equation (1) was determined on the basis of compression tests performed on the Gleeble 3800 simulator in the Institute for Ferrous Metallurgy in Gliwice. Hansel-Spittel (1979) equation was used to describe relation of the flow stress on strain, strain rate and temperature. Inverse analysis performed for the results of the compression tests gave the following values of coefficients in the Hansel-Spittel equation:

$$\sigma_p = 5843.3\varepsilon_i^{0.237}\exp(-0.347\varepsilon_i)\dot{\varepsilon}_i^{0.132}\exp(-0.00342T) \quad (2)$$

where: σ_p – flow stress, ε_i– effective strain, $\dot{\varepsilon}_i$ – effective strain rate, T – temperature in ^{o}C.

The FE heat transfer model during cooling of rails in the FE code, described by (Lenard et al., 1999), was used and it is not presented in this paper. The remaining microstructure evolution models are also described in previous publications (Kuziak et al., 1997), but they repeated briefly below.

2.2. Microstructure evolution model during rolling

Many microstructures evolution models can be found in literature. The great part of them are based on fundamental works of (Sellars, 1979) and developed by dealing with new coefficients and issues. New modelling technologies take into account not only deformation history, recrystallized volume fraction and grain size distribution but also dislocation density to predict microstructure evolution during and after hot deformation (Lin et al., 2005). These technologies allow to consider, besides microstructure evolution, also model of damage evolution process related to the inclusion size and spacing (Foster et al., 2007).

Microstructure evolution model is based on the fundamental works of (Sellars, 1979) and coefficients in this model were determined on the basis of stress relaxation tests. This model for the steel 900A was proposed first in (Kuziak et al., 1997) and the main equations are presented below:

Recrystallized volume fraction

$$X = 1-\exp\left[-0.693\left(\frac{t}{t_{0.5}}\right)^{1.7}\right] \quad (3)$$

$$t_{0.5} = 2.403\times10^{-8}\varepsilon^{-s}\dot{\varepsilon}^{-0.288}D_0^{-0.2}\exp\left[\frac{160420}{R(T+273)}\right] \quad (4)$$

$$s = 1.006D_0^{-0.2}$$

Recrystallized grain size

$$D_{RX} = 9.91\varepsilon^{-0.65}\dot{\varepsilon}^{-0.1}D_0^{0.54}\exp\left[\frac{-17540}{R(T+273)}\right] \quad (5)$$

Grain growth

$$D^2 = D_{RX}^2 + 10^A t \qquad A = 7.0-\frac{5900}{(T+273)} \quad (6)$$

where: t – time, ε – strain, $\dot{\varepsilon}$ – strain rate, D_0 – austenite grain size prior to deformation, T – temperature in ^{o}C, R – gas constant, D – austenite grain size after growth in μm.

The model was chosen to be easily implemented and integrated with numerical software and phase transformation model to predict microstructure evolution not only after hot rolling process but at the end of whole manufacturing hot rolling sequences and controlled cooling cycle.

2.3. Phase transformation model during cooling

Detailed description of the phase transformation model during cooling after rolling is given by (Pietrzyk & Kuziak, 2000; 2012). The kinetics of the pearlitic and bainitic transformations is described by the JMAK (Johnson, Mehl, Avrami, Kolmogorov) type equation:

$$X = 1-\exp(-kt^n) \quad (7)$$

where: X – transformed volume fraction, k, n – coefficients, t – time.

Equation (7) describes transient state between two equilibrium states. ThermoCalc software was used to determine equilibrium carbon concentrations in the austenite and the following relations were obtained for the investigated steel:

$$\begin{aligned} c_{\gamma\alpha} &= 4.8513-0.005776T \\ c_{\gamma\beta} &= -1.46583+0.002887T \end{aligned} \quad (8)$$

where: $c_{\gamma\alpha}$ – carbon content at the γ/α interface, $c_{\gamma\beta}$ – carbon content at the *γ/cementite* interface, T - temperature in ^{o}C.

Scheil (1935) additivity rule was applied to account for the temperature changes during transformations. Incubation time for pearlitic and bainitic transformation is accounted for.

$$\text{pearlite: } \tau_P = \frac{a_1}{(\mathrm{Ae}_1-T)^{a_3}}\exp\left[\frac{a_2\times10^3}{R(T+273)}\right] \quad (9)$$

$$\text{bainite: } \tau_b = \frac{a_9}{(a_{12}-T)^{a_{11}}}\exp\left[\frac{a_{10}\times10^3}{R(T+273)}\right] \quad (10)$$

where: T – temperature in ^{o}C, R – gas constant.

Constant value of coefficient n in equation (7) is used. The values of n are introduced in the model as a_4 and a_{13} for pearlitic and bainitic transformations, respectively. Coefficient k is defined as a temperature function:

pearlite: $$k = \frac{a_7}{D_\gamma^{a_8}} \exp\left(a_6 - \frac{a_5 T}{100}\right) \quad (11)$$

bainite: $$k = a_{17} \exp\left(a_{16} - \frac{a_{15} T}{100}\right) \quad (12)$$

where: D – grain size.

Remaining equations in the model are:

- Start temperature for bainitic transformation:

$$B_s = a_{13} - 425[\mathrm{C}] - 42.5[\mathrm{Mn}] - 31.5[\mathrm{Ni}] \quad (13)$$

- Start temperature for martensitic transformation:

$$M_s = a_{18} - a_{19} c_\gamma \quad (14)$$

Volume fraction of the martensite is calculated according to the model of Koistinen and Marburger (1959), described also in (Umemoto et al., 1992):

$$F_m = \left(1 - F_p - F_b\right)\left\{1 - \exp\left[-0.011\left(M_s - T\right)\right]\right\} \quad (15)$$

where: F_p, F_b – volume fractions of pearlite and bainite with respect to the whole volume of the sample, M_s – martensite start temperature.

Coefficients in the model for the 900A steel were determined on the basis of dilatometric tests using procedure described by (Pietrzyk et al., 2000) and are given in

Table 1. This model was connected with the FE code and was applied to simulations of controlled cooling of rails.

Table 1. *Coefficient in the phase transformation model for the 900A steel.*

a_1	a_2	a_3	a_4	a_5	a_6	a_7	a_8	a_9	a_{10}
0.0779	122.8	2.634	0.0632	0.134	8.913	0.013	0.862	1399	61.98
a_{11}	a_{12}	a_{13}	a_{14}	a_{15}	a_{16}	a_{17}	a_{18}	a_{19}	
2.537	887.6	1.083	887.6	0.942	0.399	0.386	218.1	1.646	

2.4. Model of final microstructure and properties

Details of this model are given in publications (Kuziak et al., 1997; Pietrzyk & Kuziak, 2000; 2012). The model includes equations, which describe microstructural parameters of eutectoid steel after cooling from austenite stability temperature to the room temperature. The resulting microstructure is composed of pearlite grains subdivided into colonies in the process of pearlite growth. Typically, there are several colonies in a single pearlite grain, characterized by parallel orientation of the cementite/ferrite lamellae within each colony. Pearlite microstructure composed of grains and colonies is formed when austenite grains before the transformation are relatively large (≥ 20 μm), and pearlitic transformation occurs with minor undercooling with respect to the temperature Ae_1. For smaller austenite grains and considerable undercooling of austenite at the beginning of transformation, the difference between the nodes and pearlite colonies disappears and such pearlite was called a colonial pearlite by (Garbarz & Pickering, 1988).

The spacing between cementite lamellae is the most important parameter characterizing pearlite microstructure. The surface layer of rail head is of particular interest. Fine pearlite should be a dominant component of this layer. The interlamellar spacing in pearlite, in μm, is calculated as:

$$S_0 = \frac{1}{a - bT_p}$$
$$a = 129.3 - 54.4[\mathrm{Mn}] - 4.38[\mathrm{Cr}] - 17.5[\mathrm{Si}]$$
$$b = 0.178 - 0.072[\mathrm{Mn}] - 0.012[\mathrm{Cr}] - 0.0274[\mathrm{Si}] \quad (16)$$

where: T_p – temperature of pearlitic transformation in °C, [Mn], [Cr], [Si], [C] – manganese, chromium, silicon and carbon content in wt%.

Since the temperature varies during cooling, the interlamellar spacing is calculated for weighted average temperature during the transformation. Pearlite grain size (D_p) and pearlite colony size (D_c) are two additional parameters included in the model. They are calculated from the following equations (Pietrzyk & Kuziak, 2000; 2012):

$$D_p = \frac{6500\left[1 - \exp\left(-0.016 D_\gamma\right)\right]^{0.6}}{\mathrm{Ae}_1 - T_p} \quad (17)$$

$$D_c = \frac{1}{0.857 - 0.00119 T_p} \quad (18)$$

where: T_p – average temperature of pearlitic transformation in °C.

The equations, which describe mechanical properties of eutectoid steel in the room temperature, are included in the model, as well. Yield stress ($R_{0.2}$) and tensile strength (R_m) in MPa for eutectoid steel are calculated as (Pietrzyk & Kuziak, 2012; Kuziak & Zygmunt, 2013):

$$R_{0.2} = 259 + 0.087\chi^{-1}$$

$$R_m = 793 + 0.07\chi^{-1} + 122[\mathrm{Si}] \tag{19}$$

where: $\chi = (2S_0 - t)$ – the mean free path for dislocation glide in pearlitic ferrite, t – thickness of the cementite plate calculated as $0.015S_0$[C], [Si], [C] – silicon and carbon content in wt%.

The wear resistance of pearlitic rails is directly linked with their hardness. Increasing the hardness causes the wear resistance increase. The hardness can approximately be calculated as HV = $0.27R_m$ (Kuziak & Zygmunt, 2012).

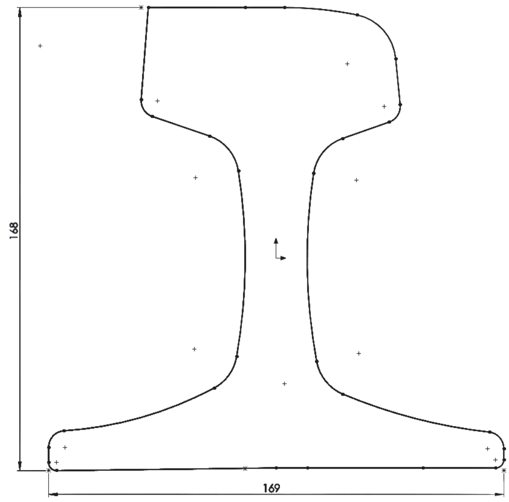

Fig. 1. Initial shape of the rail.

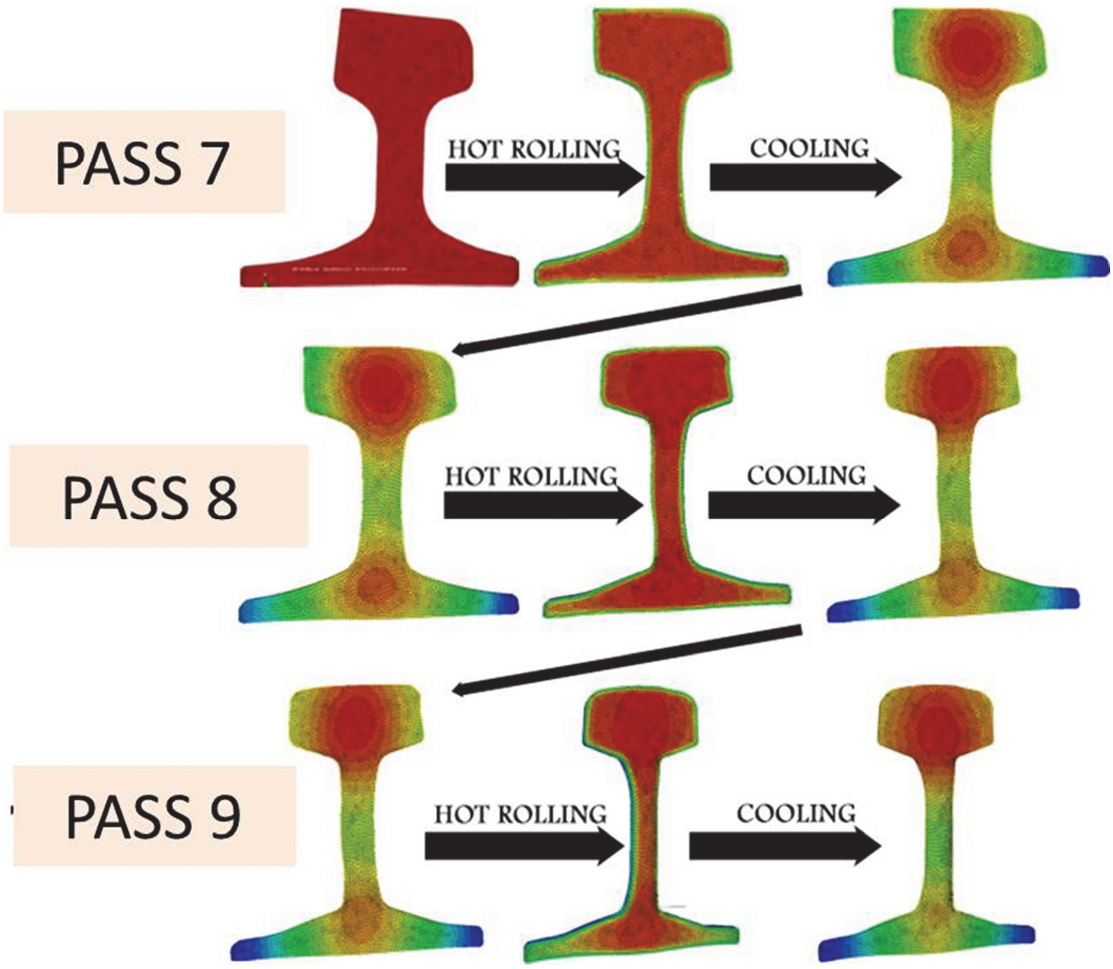

Fig. 2. Temperatura field and data transfer between the simulations of subsequent passes.

3. RESULTS

Rail rolling process involves nine passes. Due to a complex shape of the deformation zone simulation of a single pass is very time consuming. Therefore, since the microstructure of the final product is determined at the final stage of the rolling process, only last three passes of the rail rolling were considered and separated into individual problems. Each of them was divided into two sequences: hot rolling and cooling in the air after the rolling. Initial shape of rail is presented on figure 1. At the beginning of the simulation there were homogeneous temperature distribution (1000°C) and initial grail size distribution (80 μm) assumed.

Temperature, material data and FE mesh were transferred between subsequent parts of the process (figure 2) without necessity of interpolation, as it was shown by (Pei et al., 2014). Because of the full recrystallization, the strains were equalled to zero at the beginning of each individual pass. The uniform temperature distribution in the whole volume of the workpiece was assumed at the beginning of the simulation.

3.1. Hot rolling

Models of the workpiece and the rolls were prepared in the SolidWorks software and exported to Abaqus, where they were meshed and prepared for the simulation. The boundary conditions and material data have been added to the simulation of the first pass and next the data ware transferred to subsequent passes. Results are presented for a slice of elements in the central part of the sample workpiece. Thermal and mechanical parameters such as strain and stress distribution and temperature fields were calculated during the hot rolling. The results obtained for the pass 7 are shown in figure 3.

Temperature field at the entry to the 8th pass was calculated by simulation of cooling in the air between the two passes. These data were used as input to the next hot rolling pass (figure 4).

Described procedure has been repeated for each pass and the results are shown in figure 5 for the pass 8 and in figure 6 for the last pass. Since the microstructure in the rail head is of major importance, the results are presented only for this part of the cross section.

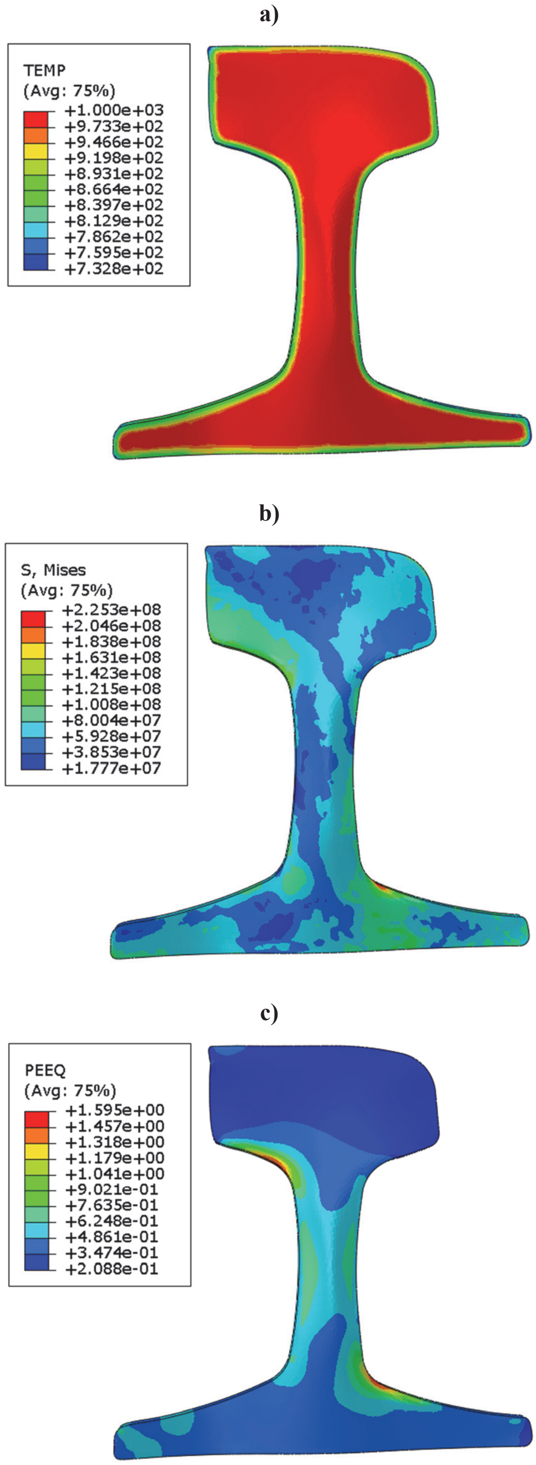

Fig. 3. *Distribution of the entry temperature (a), equivalent stress (b) and effective plastic strain (c) in the 7th pass.*

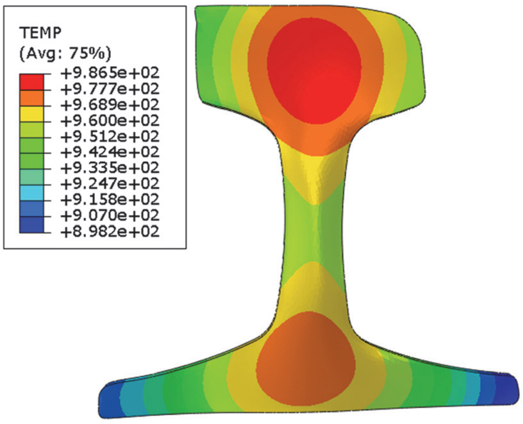

Fig. 4. Temperature field after cooling in the air after the pass 7.

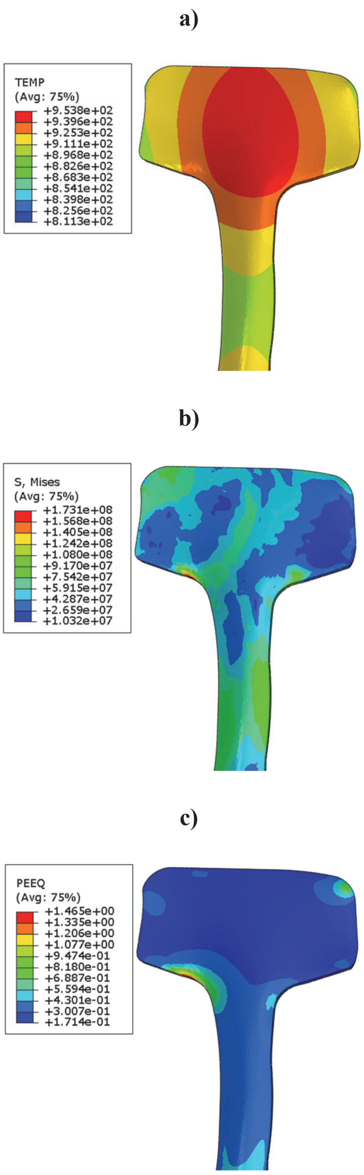

Fig. 5. Distribution of temperature (a), equivalent stress (b) and effective plastic strain (c) in the second pass.

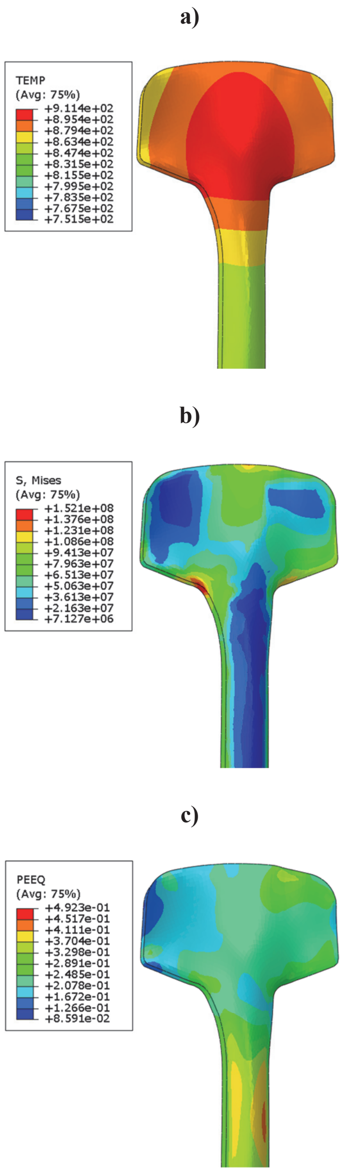

Fig. 6. Distribution of temperature (a), equivalent stress (b) and effective plastic strain (c) after the last pass.

Data from the sequences of hot rolling and cooling process were used to calculate microstructure evolution during hot rolling process. A uniform grain size for the whole volume of the rail was assumed after the 6th pass. Based on the equations (3)-(6) the changes of the austenite grain size were calculated. The results for the changes of the temperature and the grain size are presented in figure 7 for three points at the cross section of the rail head, located at the vertical axes of symmetry at the distance of 2 mm (point A), 5 mm (point B) and 26 mm (point C) from the top surface.

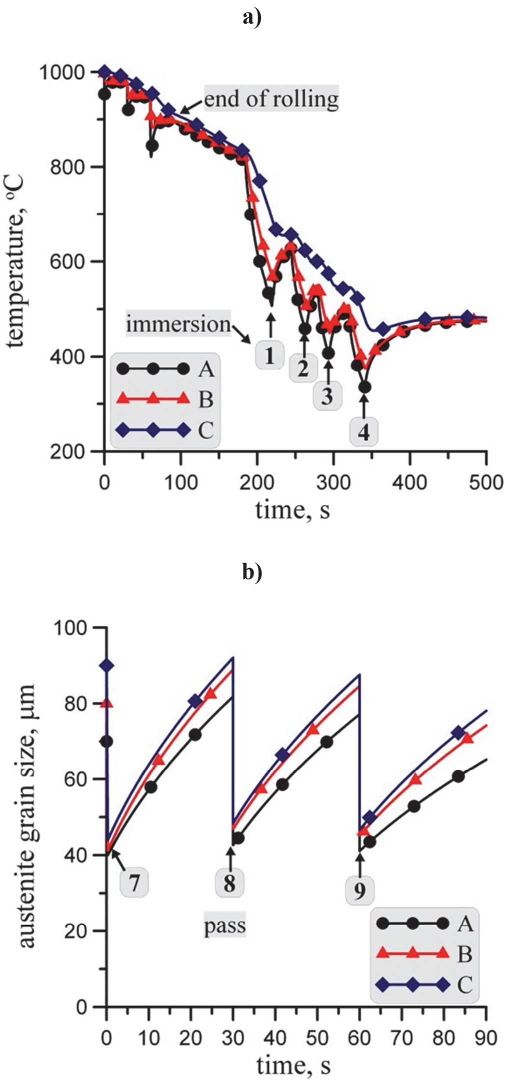

Fig. 7. Changes of the temperature (a) and the austenite grain size (b) in the three locations at the cross section of the rail head.

3.2. Laminar cooling

The system for cooling of rail head by immersion in the polymer solution was considered in the present paper. This system was proposed by (Kuziak and Zygmunt, 2012). Description of this system, as well as results of simulations of cooling, can be found in publications (Pietrzyk & Kuziak, 2012; Kuziak et al., 2014). Optimization of the cooling technology in this system was presented in (Szeliga et al., 2014).

Calculated distributions of the temperature and the austenite grain size were used as input data for further simulations of the controlled cooling. The finite element program developed at the Department of Applied Computer Science and Modelling AGH and described in (Pietrzyk & Kuziak, 2000; 2012) was used for these calculations. The process composed of four subsequent immersions of the rail head in the polymer solution was considered. Calculated changes of the temperature during cooling are shown in figure 7a as continuation of the plots obtained for the rolling process.

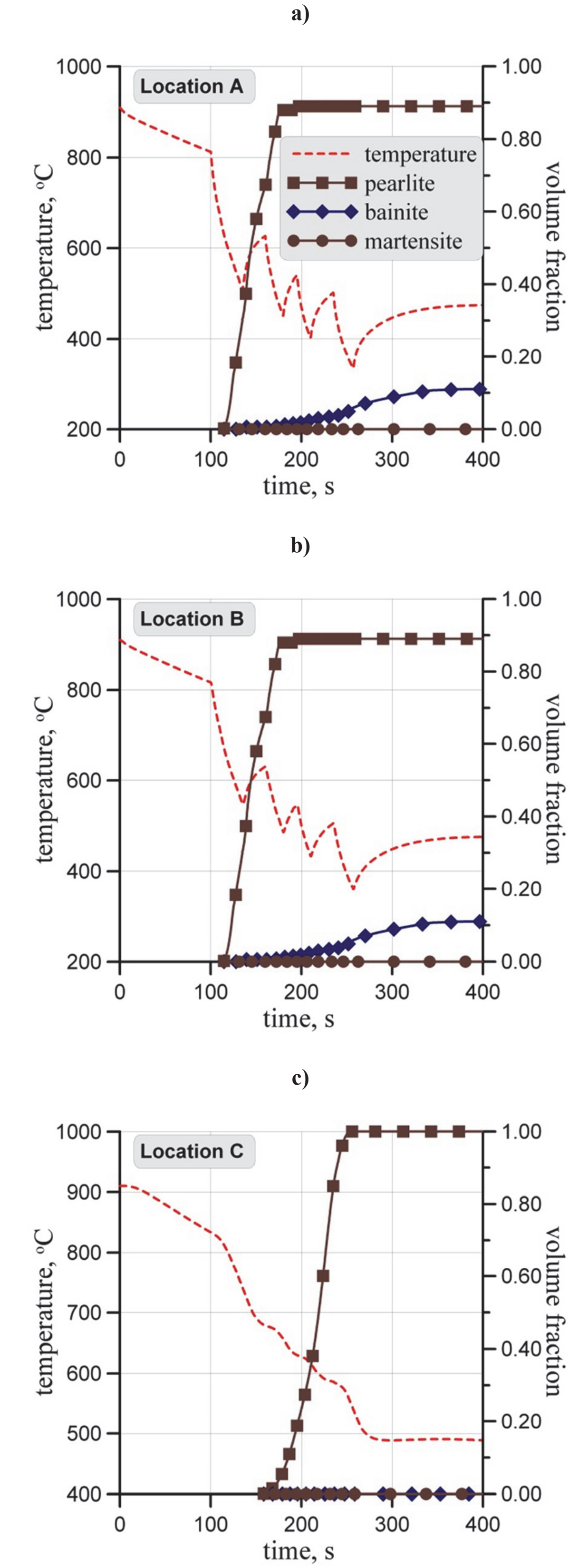

Fig. 8. Changes of the temperature and kinetics of phase transformations in three locations at the cross section of the rail head. The symbols are the same for all three plots.

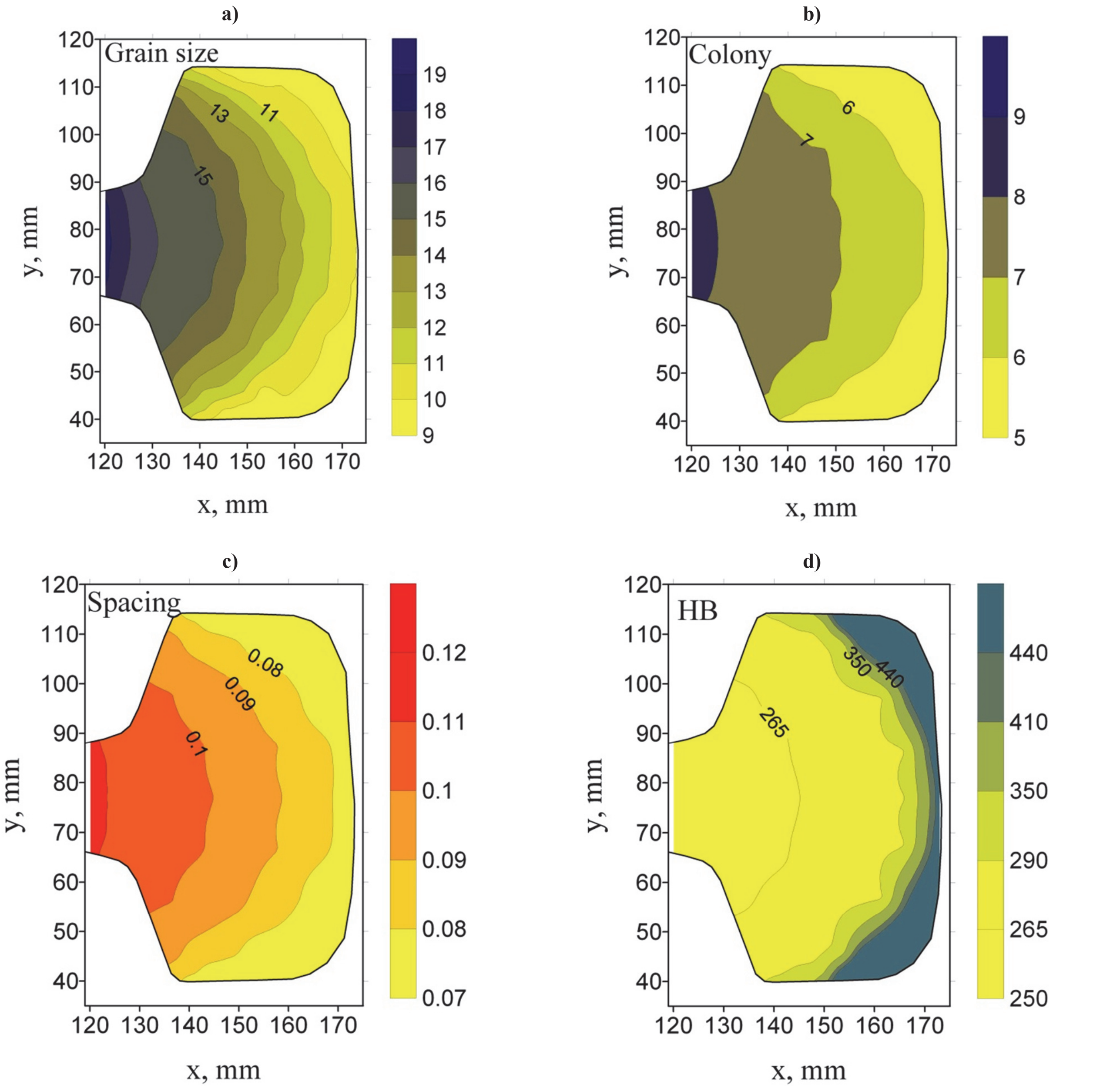

Fig. 9. *Selected results of the calculations of distributions of the pearlite grain size in μm (a), pearlite colony size in μm (b), interlamellar spacing in μm (c) and hardness HV (d).*

Results of calculations of the kinetics of phase transformation are shown in figure 8. It is seen that purely pearlitic microstructure was obtained in the central part of the rail head – the point C was located 26 mm below the surface of the rail. Figure 8a and b show that cooling of the surface of the rail head was slightly too intensive and around 10% of the bainite was predicted for the points A and B.

Since equations (16), (17) and (18) describing microstructure and equations (19) describing mechanical properties were implemented in the FE code, calculations of the distribution of these properties at the rail cross section were possible. Selected results of these calculations showing distributions of the pearlite grain size, pearlite colony size, interlamellar spacing and hardness are shown in figure 9. It is seen in this figure that due to presence of some bainite in the surface area high values of the hardness were obtained.

4. CONCLUSIONS

Microstructure evolution model and phase transformation model were implemented into the thermal-mechanical FE code and simulations of the manufacturing chain for rails were performed. Simulations confirmed good predictive capabilities of the developed program. The analysis of results allowed drawing of the following conclusions:

– Multiscale simulation of the manufacturing chain for rails is possible. Transfer of the history

dependent data (temperature distribution and microstructure distribution) between subsequent operations was developed in the paper.
- Hot rolling process for rails was simulated using Abaqus software. 3D simulations were performed and computing costs were very high. Microstructure evolution equations were solved during post processing. Results of calculations including temperature and grain size distribution were transferred to the FE thermal software for controlled cooling.
- Full coupling between thermal FE software and models describing phase transformations and product microstructure was possible. These calculations were very fast. It means that optimization of the controlled cooling process, using microstructure and properties of the product in the objective function, can be performed in an efficient way.

ACKNOWLEDGEMENTS

Financial assistance of the NCN project no. 2012/04/M/ST8/00706 is acknowledged.

REFERENCES

Ackert, R.J., Nott, M.A., 1987, Accelerated water cooling of railway rails in-line with the hot rolling mill, *Proc. Symp. Accelerated Cooling of Roled Steels*, eds, Ruddle, G.E., Crawley, A.F., Pergamon Press, Winnipeg, 359-372.

Boyadiev, I.I., Thomson, P.F., Lam, Y.C., 1996, Computation of the diffusional transformation of continuously cooled austenite for predicting the coefficient of thermal expansion in the numerical analysis of thermal stress, *ISIJ International*, 36, 1413-1419.

Foster, A.D. Lin, J., Farrugia, D.C.J., Dean, T.A., 2007, Investigation into Damage Nucleation and Growth for a Free-Cutting Steel under Hot Rolling Conditions, *Journal of Strain Analysis*, 42, 227-235.

Franklin, F.J., Gahlot, A., Fletcher, D.I., Garnham, J.E., Davis, C., 2011, Three-dimensional modelling of rail steel microstructure and crack growth, *Wear*, 271, 357-363

Garbarz, B., Pickering, F.B., 1988, Effect of pearlite morphology on impact toughness of eutectoid steel containing vanadium, *Materials Science and Technology*, 4, 328-334.

Garnham, J.E., Davis, C.L., 2011,Very early stage rolling contact fatigue crack growth in pearlitic rail steels, *Wear*, 100-112

Głowacki, M., 1996, Simulation of rail rolling using the generalized plane-strain finite-element approach, *Journal of Materials Processing Technology*, 62, 229-234.

Głowacki, M., 2000, Thermal-mechanical-microstructural model of shape rolling, *Proc. ECCOMAS Congress*, Barcelona, CD ROM.

Glowacki, M., 2005, The mathematical modelling of thermo-mechanical processing of steel during multi-pass shape rolling, *Journal of Materials Processing Technology*, 168, 336-343.

Hensel, A., Spittel, T., 1979, *Kraft- und Arbeitsbedarf Bildsamer Formgebungs-verfahren*, VEB Deutscher Verlag fur Grundstoffindustrie, Leipzig.

Koistinen, D.P., Marburger, R.E., 1959, A general equation prescribing the extent of the austenite-martensite transformation in pure iron-carbon alloys and plain carbon steels, *Acta Metallurgica*, 7, 59-69.

Kuziak, R., Cheng, Y.-W., Głowacki, M., Pietrzyk, M., 1997, Modelling of the microstructure and mechanical properties of steels during thermomechanical processing, *NIST Technical Note 1393*, Boulder.

Kuziak, R., Zygmunt, T., 2012, A new method of rail head hardening of standard-gauge rails for improved wear and damage resistance, *Steel Research International*, 84, 13-19.

Kuziak, R., Molenda, R., Wrożyna, A., Kusiak, J., Pietrzyk, M., 2014, Experimental verification and validation of the phase transformation model used for optimization of heat treatment of rails, *Computer Methods in Materials Science*, 14, 53-63.

Lenard, J.G., Pietrzyk, M., Cser, L., 1999, *Mathematical and physical simulation of the properties of hot rolled products*, Elsevier, Amsterdam.

Lin, J., Liu, Y., Farrugia, D.C.J., Zhou, M., 2005, Development of dislocation based-unified material model for simulating microstructure evolution in multipass hot rolling, *Philosophical Magazine A*, 85, 1967-1987.

Ma, J.-H, Tao B.,Yao, X.-H., 2014, Corrugated waist rail microstructure evolution simulation, *Advanced Materials Research*, 989-994, 425-428.

Morales, R.D., Lopez, A.G., Olivares, I.M., 1990, Heat transfer analysis during water spray cooling of steel rods, *ISIJ Inernational.*, 30, 48-57.

Perez-Unzueta, A.J., Beynon, J.H., 1993, Microstructure and wear resistance of pearlitic rail steels, *Wear*, 162-164, 173-182.

Pei, N.N., Zhu, G.M., Li, B., Tao, G.M., Kang, Y.L., 2014, 3D Thermo-mechanical coupled simulation of whole rolling process for 60 kg/m heavy rail. *Journal of Iron and Steel Research International*, 21, 1104-1110.

Pernach, M., 2014, Possibilities of application of numerical solution of the diffusion equation to modeling phase transformation during cooling of pearlitic steel, *Computer Methods in Materials Science*, 14, 228-235.

Pletz, M., Daves, W., Yao, W., Kubin, W., Scheriau, S., 2014,Multi-scale finite element modeling to describe rolling contact fatigue in a wheel–rail test rig, *Tribology International*, 80, 147-155.

Pietrzyk, M., Kuziak, R., 2000, Modeling of controlled cooling of rails after hot rolling, *Proc. Conf. Rolling 2000*, Vasteros, CD ROM.

Pietrzyk, M., Kondek, T., Majta, J., Zurek, A.K., 2000, Method of identification of the phase transformation model for steels, *Proc. COM 2000*, Ottawa, CD ROM.

Pietrzyk, M., Kuziak, R., 2012, Numerical simulation of controlled cooling of rails as a tool for optimal design of this process, *Computer Methods in Materials Science*, 12, 233-243.

Sahay, S.S., Mohapatra, G., Totten, G.E., 2009, Overview of pearlitic rail steels: accelerated cooling, quenching, microstructure and mechanical properties, *Journal of ASTM International*, 6, 1-26.

Scheil, E., 1935, Anlaufzeit der Austenitumwandlung, *Archiv. für Eissenhüttenwesen*, 12, 565-567.

Szeliga, D., Kuziak, R., Zygmunt, T., Kusiak, J., Pietrzyk, M., 2014, Selection of parameters of the heat treatment thermal cycle for rails with respect to the wear resistance, *Steel Research International*, 85, 1070-1082.

Umemoto, M., Hiramatsu, A., Moriya, A., Watanabe, T., Nanba, S., Nakajima, N., Anan, G., Higo, Y., 1992, Computer modelling of phase transformation from work-hardened austenite, *ISIJ International*, 32, 306-315.

Wen, Z., Wu, L., Li, L., Jin, X., Zhu, M., 2011, Three-dimensional elastic–plastic stress analysis of wheel–rail rolling contact, *Wear*, 271, 426-436.

CIEPLNO-MECHANICZNO-MIKROSTRUKTURALNY MODEL WALCOWANIA I CHŁODZENIA SZYN

Streszczenie

W artykule opisano cieplno-mechaniczno-mikrostrukturalny model walcowania i kontrolowanego chłodzenia szyn. Modele opisujące rozwój mikrostruktury i przemiany fazowe w stalach szynowych zostały zaimplementowane w programie z metody elementów skończonych, który symuluje zjawiska cieplne i mechaniczne. Przeprowadzone zostały numeryczne testy opracowanego programu. Symulacje objęły ostatnie trzy przepusty w procesie walcowania oraz proces kontrolowanego chłodzenia główki szyny po walcowaniu. W pracy przedstawiono wyniki w postaci rozkładów odkształceń i naprężeń oraz zmian temperatury w procesie walcowania, a także zmian wielkości ziarna austenitu w poszczególnych przepustach i kinetyki przemian fazowych w czasie chłodzenia. Numeryczne testy potwierdziły duże możliwości obliczeniowe modelu.

Received: May 23, 2015
Received in a revised form: September 12, 2015
Accepted: September 29, 2015